PHYSICAL REVIEW B **80**, 140405(R) (2009)

Evolution of magnetic phases and orbital occupation in $(SrMnO_3)_n/(LaMnO_3)_{2n}$ superlattices

C. Aruta,[1,*] C. Adamo,[2] A. Galdi,[1,3] P. Orgiani,[1,4] V. Bisogni,[5] N. B. Brookes,[5] J. C. Cezar,[5] P. Thakur,[5] C. A. Perroni,[1,6] G. De Filippis,[1,6] V. Cataudella,[1,6] D. G. Schlom,[2] L. Maritato,[1,4] and G. Ghiringhelli[1,7]

[1]*CNR-INFM Coherentia, Complesso Universitario di Monte Sant'Angelo, Via Cintia, I-80126 Napoli, Italy*

[2]*Department of Materials Science and Engineering, Cornell University, Ithaca, New York 14853-1501, USA*

[3]*Dipartimento di Scienze Fisiche, Università di Salerno, Baronissi, I-84081 Salerno, Italy*

[4]*Dipartimento di Matematica ed Informatica, Università di Salerno, Baronissi, I-84081 Salerno, Italy*

[5]*European Synchrotron Radiation Facility, Boîte Postale 220, F-38043 Grenoble, France*

[6]*Dipartimento di Scienze Fisiche, Università di Napoli Federico II, Complesso Universitario di Monte Sant'Angelo, Via Cintia, I-80126 Napoli, Italy*

[7]*Dipartimento di Fisica, Politecnico di Milano, Piazza Leonardo da Vinci 32, I-20133 Milano, Italy*

(Received 3 July 2009; revised manuscript received 30 August 2009; published 9 October 2009)

The magnetic and electronic modifications induced at the interfaces in $(SrMnO_3)_n/(LaMnO_3)_{2n}$ superlattices have been investigated by linear and circular magnetic dichroism in the Mn $L_{2,3}$ x-ray absorption spectra. Together with theoretical calculations, our data demonstrate that the charge redistribution across interfaces favors in-plane ferromagnetic (FM) order and $e_g(x^2-y^2)$ orbital occupation, in agreement with the average strain. Far from interfaces, inside $LaMnO_3$, electron localization and local strain favor antiferromagnetism (AFM) and $e_g(3z^2-r^2)$ orbital occupation. For $n=1$ the high density of interfacial planes ultimately leads to dominant FM order forcing the residual AFM phase to be in-plane too, while for $n \geq 5$ the FM layers are separated by AFM regions having out-of-plane spin orientation.

DOI: 10.1103/PhysRevB.80.140405 PACS number(s): 75.47.Lx, 72.10.Di, 73.21.Cd, 78.70.Dm

Interfaces between different transition-metal oxides (TMOs) have been widely demonstrated to be sources of interesting and unexpected electronic and magnetic properties. Metallic conductivity arises, for example, at the interface between two insulators, such as $LaAlO_3/SrTiO_3$ (Ref. 1) and $LaTiO_3/SrTiO_3$ (Ref. 2) while ferromagnetism (FM) occurs at the interface between the antiferromagnet (AFM) $CaMnO_3$ and the paramagnet $CaRuO_3$.[3] In this context, strain driven spin-orbital coupled states arising in manganites make the interfaces between these compounds very interesting for engineering unique collective states. As a matter of fact, a certain amount of theoretical and experimental studies on superlattices (SLs) composed by the two AFM insulators, $SrMnO_3$ (SMO) and $LaMnO_3$ (LMO), appeared in literature during the last years.[4–12] The ordered sequence of the atomic layers in the digital SMO/LMO SLs,[4,5] together with the electronic reconstruction arising from the interfacial Mn^{3+}/Mn^{4+} mixed valence, give rise to peculiar transport, magnetic and orbital properties, when different layering and strain conditions occur. In the particular case of $(SMO)_n/(LMO)_{2n}$ the La:Sr ratio is 2:1, in analogy with the optimal composition of $La_{2/3}Sr_{1/3}MnO_3$ (LSMO). In such a case, the metal-insulator transition (MIT) and the magnetic properties depend on the thickness of the constituent blocks,[4–7] although in a nontrivial way. Indeed, saturation magnetization does not linearly decrease with n (Ref. 4) and both fast and viscous spin populations are present, the latter associated to FM/AFM pinning.[8] Therefore, the development of the FM metallic phase at the interfaces is well established and the coexistance of the FM and AFM phases was inferred. However, the knowledge of the mutual dependence of the AFM and FM phases with n is still uncertain, but it could open further perspectives in the control of the low dimensional magnetic properties, thus in the engineering of the TMO magnetic heterostructures. In addition, as the role of interfacial Mn e_g electrons is known to be important, the influence of strain and reduced dimensionality on the transport properties requires some attention.[6,7,9,10] In the case of LMO/SMO SLs the two materials widely change their behavior with respect to bulk. So, while in bulk the e_g levels of SMO are empty and LMO presents in-plane $(x^2-r^2)/(y^2-r^2)$ orbital order, at SMO/LMO interfaces strain and electronic reconstruction are expected to modify orbital population and ordering in both components.[11,12]

We have determined the orbital and magnetic properties of $(SMO)_n/(LMO)_{2n}$ SLs with $n=1$, 5, and 8 by measuring x-ray *linear* dichroism (XLD) and *magnetic circular* dichroism (XMCD) in x-ray absorption spectra (XAS) at the Mn $L_{2,3}$ edge. Thanks to our experimental techniques, we have been able to follow the evolution with n of the FM and AFM phases along with the preferred e_g level orbital occupation. We have found that the AFM spin direction is aligned with the FM easy-axis direction for $n=1$, while is perpendicular to it for $n=5$ and 8, and that the preferential orbital occupation is of the $e_g(x^2-y^2)$ type for $n=1$ and of the $e_g(3z^2-r^2)$-type for $n=5$ and 8. We discuss these experimental results in terms of the role played in the system by the charge-carrier delocalization and the epitaxial strain.

The measurements have been performed at the beamline ID08 of the European Synchrotron Radiation Facility (Grenoble, France), which is based on AppleII undulator source (allowing a full control of linear and circular polarization) and a high scanning speed spherical grating monochromator (Dragon type). The absorption signal has been measured in total electron yield. A magnetic field parallel to the incident beam was provided by a superconducting electromagnet. The XMCD signal is proportional to the atomic magnetic moments in ferromagnetically ordered samples.[13] On the contrary XLD can be due to an orbital or magnetic uniaxial anisotropy (or both), and the magnetic part (XMLD,

x-ray *magnetic linear* dichroism) is sensitive to both FM and AFM ordering.[14] To disentangle the magnetic from the orbital part of XLD we have performed measurements at different temperatures T: above the magnetic ordering temperature only the orbital contribution survives, so in our samples XLD at high T (room T for $n=1$ and 200 K for $n=5$ and 8) have orbital character only. This orbital XLD is due to the uneven population of the two e_g orbitals $[(3z^2-r^2)$ and $(x^2-y^2))]$ at Mn^{3+} sites. To obtain the purely magnetic XMLD signal at low T (10 K), we have subtracted the XLD_{HighT} from the XLD_{LowT}, under the hypothesis that the orbital XLD does not depend on T. Moreover, using a strong (1 T) magnetic field parallel to the incident beam, the FM moments can be fully aligned so that they do not contribute to XMLD, and the pure AFM contribution to XMLD can be measured.[15]

The investigated samples were all grown on $SrTiO_3$ (STO) substrates and with a total thickness of 200 Å.[4] The crystallographic structures of the SMO and LMO constituent blocks are different, between them and with respect to the STO substrate. As a consequence, the $(SMO)_n/(LMO)_{2n}$ SLs epitaxially grown on STO experience a modulated strain, with the SMO and LMO layers being in-plane compressed and tensile extended, respectively. In particular, bulk LMO is an A-type AFM (Ref. 16) and the room-temperature crystal structure belongs to the orthorhombic space group $Pbnm$ with lattice constants $a=5.537$ Å, $b=5.747$ Å, and $c=7.693$ Å.[17] Bulk SMO is a G-type AFM (Ref. 18) and the cubic lattice cell belongs to the $Pm3m$ (Ref. 19) space group with lattice parameter $a=3.805$ Å. Both LMO and SMO films try to release the stress energy induced by the large lattice mismatch between the film and substrate and partially relax their epitaxial strain. Indeed, our 200 Å thick films of LMO and SMO on STO substrate have shown c-axis values about 3.93 and 3.78 Å, respectively. Very strained interfaces are therefore formed in the SLs, where the FM phase nucleates and starts to propagate far from the interfaces in the AFM constituent blocks. Such interfacial FM phase is detected in all investigated samples by the XMCD measurements of Fig. 1, which is added to some FM content of the LMO block already discussed in literature.[4,5]

In Fig. 1(b) the hysteresis loops in grazing-incidence (GI) and normal-incidence (NI) configurations are also reported. It can be observed that FM easy axis is mostly oriented in the ab plane. This FM anisotropy resembles that one induced by the magnetocrystalline anisotropy in the LSMO films under tensile strain.[20] The most interesting result is that the anisotropy ratio is larger in the SL with $n=1$, where the density of FM interfaces is highest, and decreases with n. Large hysteresis cycles as in our $n=5$ and $n=8$, already reported in literature for the $n=2$, 3, and 5,[8] were explained in terms of competing AFM/FM interactions with magnetic pinning, frustration and canted order. Somehow more surprising is that in all samples we find an important AFM contribution to XLD as shown in Fig. 2. As explained above, for $B=0$ T both FM and AFM phases contribute to XMLD whereas for $B=1$ T the signal is coming only from the AFM phase. For $n=5$ and 8 and for pure LMO (not shown) XMLD(0 T) and XMLD(1 T) have similar shape but opposite sign, while for $n=1$ they have the same sign. This means[21,22] that in the former cases the FM and AFM phases have magnetic moments oriented in (roughly) orthogonal directions, but are approximately parallel for $n=1$. Therefore, as the FM easy axis is mostly in-plane in all our samples (as confirmed by XMCD measurements of Fig. 1), we can conclude that the AFM easy axis is in-plane for $n=1$ and out-of-plane in the other SLs. Out-of-plane local spin AFM direction has been also observed on LMO single films (not shown). We notice from Fig. 2 that XMLD (1T) is weaker for $n=1$ and it increases with n, indicating that the fraction of AFM phase increases when reducing the interface density. In Fig. 2(b) we summarize these information by plotting the integral of the XMLD spectra at $B=1$ T. Observing that for $n=1$ the single SrO layers are sandwiched between two interfaces, namely the interfacial MnO_2 planes, the intrinsic properties of SMO block are not recovered. On the contrary, for bigger values of n an AFM contribution from the SMO layer could survive, as it has been theoretically predicted by Nanda and Satpathy[7] together with a contribution from the LMO block. Also in several experimental works[5,23,24] the AFM region has been located in the SMO blocks too. The schematic drawing on the right side of Fig. 2 depicts that, for very thin constituent blocks such as $n=1$, the AFM local spin direction is pinned to a mainly in-plane orientation by the interfacial FM anisotropy. The AFM content is responsible for the reduced Bohr magnetons number in SL $n=1$, about $3.0\mu_B/Mn$ (Ref. 4) compared with the optimal $3.7\mu_B/Mn$ value of the LSMO films.[25] When increasing the constituent blocks thickness the AFM phase might remain oriented in-plane only very close to FM interface, while it keeps the out-of-plane anisotropy far from the interfaces.

A further insight in the SLs properties comes from the XLD spectra above the magnetic ordering temperature. The XLD spectra of Fig. 3 show that for $n=5$ and $n=8$ the preferential orbital occupation is the same of pure LMO on STO:

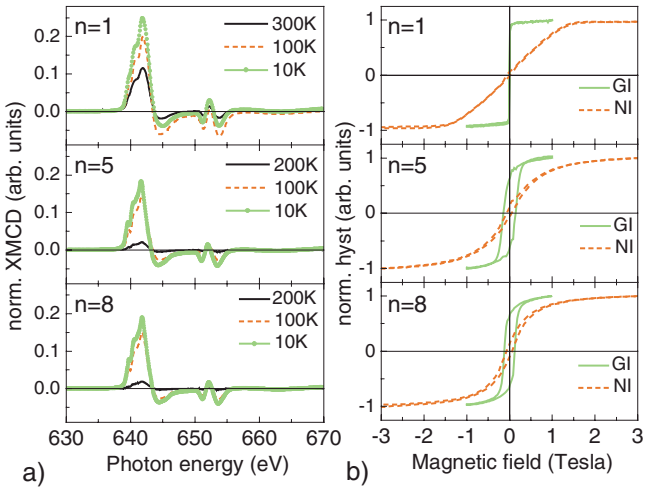

FIG. 1. (Color online) (a) XMCD results at grazing incidence with an applied magnetic field of 1 T and at different temperatures for SLs with $n=1$, 5, and 8. The XMCD results are normalized to the sum of the XAS L_3 peak height signals (b) Hysteresis loops at 10 K obtained by the maximum peak intensity of the XMCD (about 642 eV) as a function of the applied magnetic field. The curves are normalized to unity for a better comparison of the coercive fields.

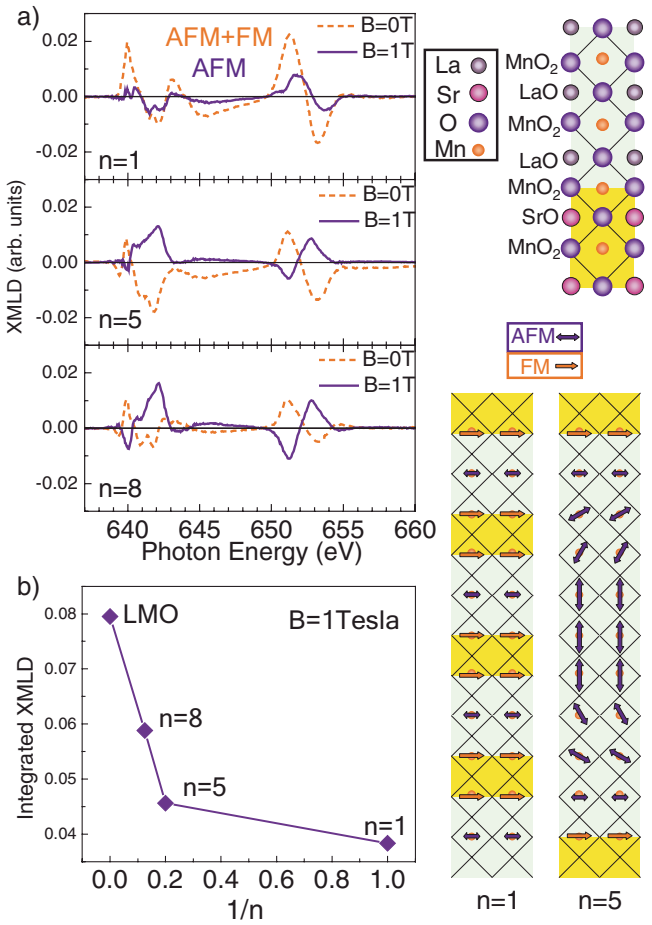

FIG. 2. (Color online)(a) Difference between the XLD spectra taken at 10 K and 300 ($n=1$) or 200 K ($n=5,8$), with $B=0$ T and $B=1$ T. All spectra are normalized to the sum of the XAS L_3 peak height signals. (b) Integral of the curves at $B=1$ T with respect to $1/n$. On the right, the schematic drawing of the local spin orientation in the superlattices is reported. The length of the arrows is roughly proportional to the magnetic (AF or AFM) content of the MnO_2 layers.

out-of-plane e_g orbitals $[3z^2-r^2$ or $(y^2-z^2)/(z^2-x^2)]$ are preferentially occupied, in analogy to what has been found for LSMO films under compressive strain.[26,27] Moreover, we observe that the XLD amplitude grows with increasing n, i.e., with decreasing interface density. On the contrary, for the metallic $n=1$ SL the XLD signal, although weaker, is clearly reversed in sign with respect to the other cases, indicating an in-plane preferential orbital occupation, possibly with $e_g(x^2-y^2)$ symmetry.[26,28]

These results can be understood starting from the following observations. First all superlattices are coherently strained: all of them are forced to the in-plane lattice parameter a of the STO substrate and to an average out-of-plane parameter $c \simeq 3.87$ Å,[4] thus giving $c/a<1$ in average. As a consequence, the LMO blocks are subjected to compressive strain (−2.2%) and the SMO blocks to tensile strain (+2.6%). Furthermore, the orbital contribution to the XLD for $n=5$ and $n=8$ is mainly given by the LMO layer since in those SLs the Mn sites in SMO layers are essentially $3d^3$, a configuration that is spherical and cannot contribute significantly to XLD. Calculations of the spatial charge density for the three superlattices (Fig. 4) indicate that the e_g levels of Mn^{4+} in SMO are generally not occupied apart from a narrow region at the interface. On the contrary, the compressive strain on LMO block of the SLs, where Mn is $3d^4$, stabilizes the $(3z^2-r^2)$ orbitals, leading to a dichroic signal similar to that of LMO alone. The results of Fig. 4 are based on density calculations made within a self-consistent Hartree approach

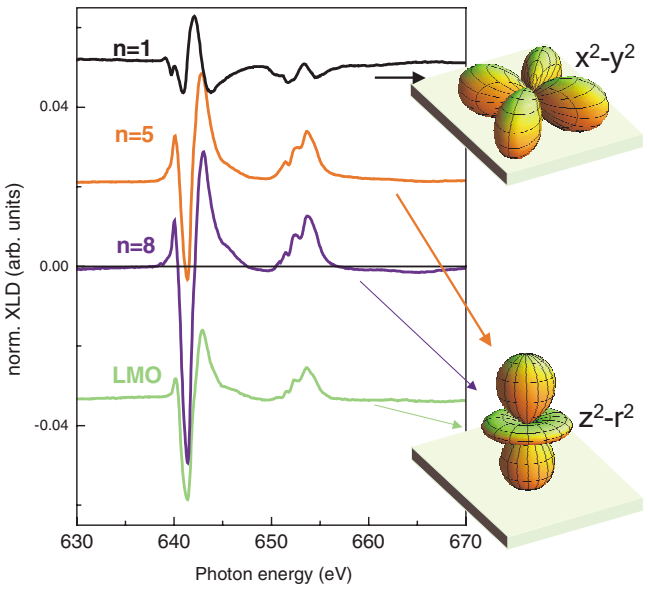

FIG. 3. (Color online) XLD spectra at 300 K for $n=1$ SL and 200 K for $n=5$ and 8 SLs and the LMO film. The spectra are reported as the difference of the XAS measurements with vertical (v) and horizontal (h) polarizations in grazing incidence configuration and normalized to the sum of the XAS L_3 peak height signals.

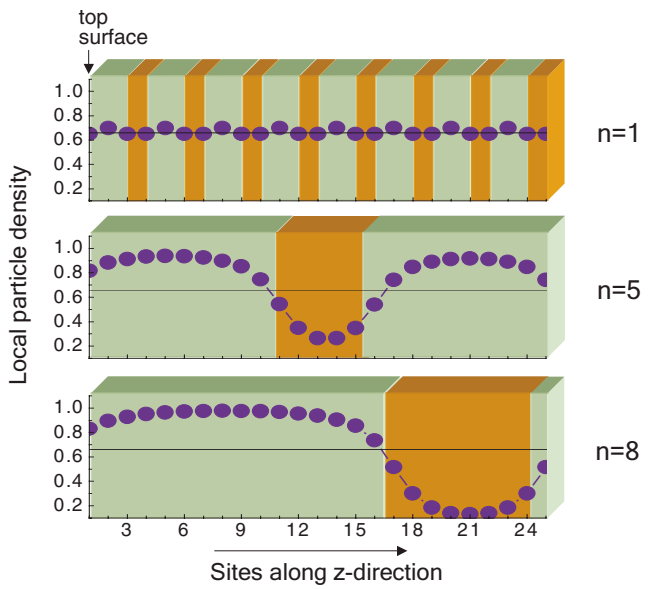

FIG. 4. (Color online) Schematic drawing of the top part of SLs measured by total electron yield, together with the spatial charge density (blue dots) along the samples, calculated as described in the text. Green (light) and orange (dark) zones represent LMO and SMO constituent blocks, respectively.

for the SL configurations (see also Refs. 6 and 9), and on the results of Ref. 10. The previous arguments can also explain the stronger XLD signal in the $n=8$ SL with respect to the $n=5$ case. In the latter case, in fact, the e_g electron-density distribution, as shown in Ref. 10, shows a small reduction in the LMO region and an increase in the SMO (see again Fig. 4). The former reduces the $e_g(3z^2-r^2)$ signal while the latter, subjected to tensile strain, contributes with a very small $e_g(x^2-y^2)$ component. For $n=1$ the situations is completely different. The contributions from LMO and SMO blocks cannot any longer be distinguished, the e_g electron-density distribution becomes almost constant (see Fig. 4) and equal to the average density. The strain does not act in opposite way on LMO and SMO, but the system responds as a whole to the average strain that is slightly tensile, and the $e_g(x^2-y^2)$ orbitals get stabilized as in LSMO grown on STO (Refs. 26 and 28) or in $(LMO)_1/(SMO)_1$ SLs.[12]

In conclusion, our study demonstrate that when the charge transfer through the interfaces delocalize the e_g electrons into the entire SL, the $n=1$ SL behaves as an homogeneous system. On the contrary, when the interface density is smaller ($n=5,8$) and the distance between interfaces is higher than the Thomas-Fermi length,[5,9] the role played by the strain applied to each constituent block becomes fundamental. As a consequence the electronic localization is accompanied by the preferential out-of-plane orbital occupation. Moreover the in-plane easy axis of the double-exchange FM spin orientation, with the pinned AFM spin orientation, further confirms that the uniform electronic distribution in the $n=1$ SL causes properties dominated by the average strain effects as a whole, thus favoring the in-plane orbital occupation. However, when the thickness of the constituent blocks increases the interfacial FM phase does not extent in the whole superlattices and the AFM spin direction starts to rotate toward the out-of-plane direction.

C. Aruta acknowledges the ESF activity Thin Films for Novel Oxide Devices (THIOX), within the Exchange Grants program.

*aruta@na.infn.it

[1] A. Ohtomo and H. Y. Hwang, Nature (London) **427**, 423 (2004).
[2] A. Ohtomo, D. A. Muller, J. L. Grazul, and H. Y. Hwang, Nature (London) **419**, 378 (2002).
[3] K. S. Takahashi, M. Kawasaki, and Y. Tokura, Appl. Phys. Lett. **79**, 1324 (2001).
[4] C. Adamo, X. Ke, P. Schiffer, A. Soukiassian, M. Warusawithana, L. Maritato, and D. G. Schlom, Appl. Phys. Lett. **92**, 112508 (2008).
[5] A. Bhattacharya, S. J. May, S. G. E. te Velthuis, M. Warusawithana, X. Zhai, B. Jiang, J.-M. Zuo, M. R. Fitzsimmons, S. D. Bader, and J. N. Eckstein, Phys. Rev. Lett. **100**, 257203 (2008).
[6] Shuai Dong, Rong Yu, Seiji Yunoki, Gonzalo Alvarez, J.-M. Liu, and Elbio Dagotto, Phys. Rev. B **78**, 201102(R) (2008).
[7] B. R. K. Nanda and S. Satpathy, Phys. Rev. B **79**, 054428 (2009).
[8] H. B. Zhao, K. J. Smith, Y. Fan, G. Lüpke, A. Bhattacharya, S. D. Bader, M. Warusawithana, X. Zhai, and J. N. Eckstein, Phys. Rev. Lett. **100**, 117208 (2008).
[9] C. Lin and A. J. Millis, Phys. Rev. B **78**, 184405 (2008).
[10] C. Adamo, C. A. Perroni, V. Cataudella, G. De Filippis, P. Orgiani, and L. Maritato, Phys. Rev. B **79**, 045125 (2009).
[11] H. Yamada, M. Kawasaki, T. Lottermoser, T. Arima, and Y. Tokura, Appl. Phys. Lett. **89**, 052506 (2006).
[12] B. R. K. Nanda and Sashi Satpathy, Phys. Rev. B **78**, 054427 (2008).
[13] J. Stöhr, J. Electron Spectrosc. Relat. Phenom. **75**, 253 (1995).
[14] D. Alders, J. Vogel, C. Levelut, S. D. Peacor, M. Sacchi, T. Hibma, L. H. Tjeng, C. T. Chen, G. van der Laan, B. T. Thole, and G. A. Sawatzky, Europhys. Lett. **32**, 259 (1995).
[15] C. Aruta, G. Ghiringhelli, V. Bisogni, L. Braicovich, N. B. Brookes, A. Tebano, and G. Balestrino, Phys. Rev. B **80**, 014431 (2009).
[16] E. O. Wollan and W. C. Koehler, Phys. Rev. **100**, 545 (1955).
[17] J. Rodrìguez-Carvajal, M. Hennion, F. Moussa, A. H. Moudden, L. Pinsard, and A. Revcolevschi, Phys. Rev. B **57**, R3189 (1998).
[18] T. Takeda and S. Ohara, J. Phys. Soc. Jpn. **37**, 275 (1974).
[19] O. Chmaissem, B. Dabrowski, S. Kolesnik, J. Mais, D. E. Brown, R. Kruk, P. Prior, B. Pyles, and J. D. Jorgensen, Phys. Rev. B **64**, 134412 (2001).
[20] T. K. Nath, R. A. Rao, D. Lavric, C. B. Eom, L. Wu, and F. Tsui, Appl. Phys. Lett. **74**, 1615 (1999).
[21] J. Fujii, F. Borgatti, G. Panaccione, M. Hochstrasser, F. Maccherozzi, G. Rossi, and G. van der Laan, Phys. Rev. B **73**, 214444 (2006).
[22] A. A. Freeman, K. W. Edmonds, G. van der Laan, N. R. S. Farley, T. K. Johal, E. Arenholz, R. P. Campion, C. T. Foxon, and B. L. Gallagher, Phys. Rev. B **73**, 233303 (2006).
[23] S. J. May, A. B. Shah, S. G. E. teVelthuis, M. R. Fitzsimmons, J. M. Zuo, X. Zhai, J. N. Eckstein, S. D. Bader, and A. Bhattacharya, Phys. Rev. B **77**, 174409 (2008).
[24] S. Smadici, Peter Abbamonte, Anand Bhattacharya, Xiaofang Zhai, Bin Jiang, Andrivo Rusydi, James N. Eckstein, Samuel D. Bader, and Jian-Min Zuo, Phys. Rev. Lett. **99**, 196404 (2007).
[25] P. Orgiani, A. Yu. Petrov, C. Adamo, C. Aruta, C. Barone, G. M. De Luca, A. Galdi, M. Polichetti, D. Zola, and L. Maritato, Phys. Rev. B **74**, 134419 (2006).
[26] C. Aruta, G. Ghiringhelli, A. Tebano, N. G. Boggio, N. B. Brookes, P. G. Medaglia, and G. Balestrino, Phys. Rev. B **73**, 235121 (2006).
[27] A. Tebano, C. Aruta, P. G. Medaglia, F. Tozzi, G. Balestrino, A. A. Sidorenko, G. Allodi, R. De Renzi, G. Ghiringhelli, C. Dallera, L. Braicovich, and N. B. Brookes, Phys. Rev. B **74**, 245116 (2006).
[28] C. Aruta, G. Balestrino, A. Tebano, G. Ghiringhelli, and N. B. Brookes, EPL **80**, 37003 (2007).